

Title	Ultrahigh-sensitive wireless QCM with bio-nanocapsules
Author(s)	Noi, Kentaro; Iijima, Masumi; Kuroda, Shun'ichi et al.
Citation	Sensors and Actuators B: Chemical. 2019, 293, p. 59-62
Version Type	AM
URL	https://hdl.handle.net/11094/84135
rights	© 2019 Elsevier B.V. This manuscript version is made available under the Creative Commons Attribution-NonCommercial-NoDerivatives 4.0 International License.
Note	

Osaka University Knowledge Archive : OUKA

<https://ir.library.osaka-u.ac.jp/>

Osaka University

Ultrahigh-Sensitive Wireless QCM with Bio-nanocapsules

Kentaro Noi^a, Masumi Iijima^b, Shun'ichi Kuroda^c, Hirotsugu Ogi^{a*}

^a *Graduate School of Engineering, Osaka University
Yamadaoka 2-1, Suita, Osaka 565-0871, Japan*

^b *Faculty of Applied Bioscience, Tokyo University of Agriculture
Setagaya-ku, Tokyo 156-8502, Japan*

^c *The Institute of Scientific and Industrial Research
Osaka University, Osaka 567-0047, Japan*

Abstract

Quartz-crystal-microbalance (QCM) biosensor is a mass-sensitive biosensor, and its sensitivity in detecting target proteins can be improved with weighted detection antibodies. In this communication, we propose a mass-amplified detection of biomarkers by bio-nanocapsules (BNCs) in wireless high-frequency multichannel QCM biosensor. BNC exhibits molecular mass of 6.57 MDa and possesses many immunoglobulin-G (IgG) Fc-binding Z domains on its surface, making it possible to display ~ 60 antibodies in an oriented immobilization manner. We find that by reinforcing the bond strength between the Z domain and the Fc part of antibody with the cross-linker, a high sensitive detection of biomarkers with QCM is realized. We used multichannel wireless QCM system with fundamental resonance frequencies above 54 MHz and performed detection of C-reactive protein. The detection limit is lower than 10 pg/mL, confirming that combination of BNC and wireless high-frequency QCM allows high sensitivity detection of biomarkers.

Keywords: QCM, bio-nanocapsule, multichannel, wireless, CRP

1. Introduction

The quartz-crystal microbalance (QCM) biosensor [1, 2, 3] is a representative label-free biosensor. It recognizes target biomolecules through the mass addition, which is detected by decrease in the resonance frequency. Because

of this simple measurement configuration, QCM biosensor allows compact apparatus and field monitoring, which would be uneasy with other label-free biosensors. There are two approaches in improving the mass sensitivity of a QCM biosensor. First is thinning the quartz resonator. Because the QCM mass sensitivity is inversely proportional to square of resonator thickness [4], QCM biosensor systems with thinner resonators have been intensively developed [5, 6, 7], where our wireless-electrodeless technique largely improved the QCM sensitivity [4]. Second is the mass-amplified sandwich assay. It is possible to amplify the frequency response after capturing target materials by injecting the mass-amplified detection materials, which bind to the targets. In such sandwich assays, gold nanoparticles have been widely used as the weight label [8, 9, 10], and protein-based mass amplification is also proposed [11]. In these mass-amplification methods, the orientation control on detection antibody is difficult, and overcoming this difficulty will make the mass-amplification approach more effective.

In this study, we propose to combine a wireless high-frequency QCM and bio-nanocapsules (BNCs) for high-sensitive detection of biomarkers. The wireless-QCM biosensor inherently shows higher mass sensitivity than conventional QCM biosensors with fundamental resonance frequencies of ~ 10 MHz or lower, because it allows us to use thinner quartz resonators with thicknesses of $\sim 30 \mu\text{m}$ or less [4]. For oriented immobilization of detection antibody molecules, we use BNC with the tandem-form IgG Fc-binding Z domain derived from *Staphylococcus aureus* protein A (ZZ-BNC) [12, 13]. The ZZ-BNC shows molecular mass of 6.57 MDa, and it is capable of capturing about 60 IgG molecules [12], so that totally a hundredfold mass amplification is expected. IgG molecules captured by the ZZ-BNC are also highly oriented so that their antigen-recognition Fv regions can face outwardly [12]. Furthermore, IgG molecules on BNC surface cause flexibly rotational Brownian motion, which enhances the binding affinity to the corresponding antigen [13]. Thus, this combination will allow us to make an ultra-sensitive detection of biomarkers. We demonstrate this proposal using C-reactive protein (CRP) as a model target.

2. Experimental Section

2.1. Multichannel wireless QCM

We used the multichannel wireless QCM biosensor[14], where three or two rectangular parallelepiped AT-cut quartz resonators ($2.5 \times 1.7 \text{ mm}^2$ area)

with slightly different fundamental resonance frequencies between 54 and 60 MHz were set. They were packaged in the microchannel fabricated in the silicon-robber gaskets by sandwiching their corners lightly by the gaskets as shown in Fig. 1. Their vibrations were simultaneously excited by the driving line antenna, and the reverberating vibrating signals were detected by the detection antenna contactlessly. The different sensor response of each channel can be independently detected because of the different resonance frequency. Details of the measurement principle [14] and the electronics [15] appear elsewhere.

2.2. Kinetics measurement between CRP and anti-CRP antibodies

We first confirmed the kinetics between CRP (HyTest Ltd. #8C72) and anti-CRP antibodies. We used two anti-CRP antibodies for capturing CRP on the sensor surface (HyTest Ltd. #4C28-C2) and for detecting CRP together with ZZ-BNC (HyTest Ltd. #4C28-C6). We call them ACRP-C2 and ACRP-C6, respectively. Before packaging the resonators, we deposited 5-nm Cr and then 15-nm Au thin films on both surfaces of each resonator. Their surfaces were first washed with piranha solution (98% H_2SO_4 :33% H_2O_2 =7:3). After rinsing them with ultrapure water, their surfaces were cleaned with a UV ozone cleaner. The resonators were then immersed in 10 mM 10-carboxy-1-decanethiol (Dojindo, #C385) solution for 12 h at 4 °C. After rinsing them with ultrapure water, their surfaces were activated by 100 mM EDC(1-ethyl-3-(3-dimethylaminopropyl)carbodiimide, hydrochloride (Dojindo, #W001) solution and 100 mM NHS (N-Hydroxysuccinimide) (Wako, #089-04032) solution for 1 h. After rinsing with ultrapure water, the resonators were immersed in 200 $\mu\text{g}/\text{ml}$ CRP in phosphate buffered saline (PBS) solution for 12 h at 4 °C for immobilizing the CRP molecules on the surfaces. After washing with ultrapure water, they were immersed in 10 mg/ml bovine-serum-albumin (BSA) (Sigma, #A3059-10G) solution for blocking remaining activated sites. After washing with PBS, we packaged the resonators in the flow channel and injected 10 $\mu\text{g}/\text{ml}$ ACPR-C6 or ACRP-C2 solution with a flow rate of 100 $\mu\text{l}/\text{min}$.

2.3. Sandwich assay with mass-amplified detection antibody

We immobilized ACRP-C2 on the resonator surfaces as the capturing antibody with the same procedure as above, and, after the blocking procedure with the BSA solution, we immersed the resonators in CRP solutions with various concentrations for 1 h at room temperature. One of the resonators

was used as a reference channel, on which CRP was not reacted. The resonators were then packaged in the flow channel and the mass-amplified anti-CRP antibody solution (shown below) was injected with a flow rate of 100 $\mu\text{l}/\text{min}$.

2.4. Preparation of ZZ-BNC solution for mass-amplified detection

We first mixed 4 $\mu\text{g}/\text{ml}$ ZZ-BNC solution with 20 $\mu\text{g}/\text{ml}$ ACRP-C6 solution to obtain total mixture solution of 2.5 ml. (The Fc parts of the anti-CRP antibody and the Fc-binding Z domain on the ZZ-BNC interact with each other in this solution.) We then added the cross-linker solution, containing 12.5 mM bis(sulfosuccinimidyl) suberate (BS^3) (DOJINDO, #B574) in PBS, for making the bonds between the Z domains and the Fc parts tightened as illustrated in Fig. 2. We then added 1 M Tris-HCl at pH8.0 for stopping the cross-linking reaction. We added finally PBS solution to obtain final concentrations of 2 $\mu\text{g}/\text{ml}$ ZZ-BNC and 10 $\mu\text{g}/\text{ml}$ ACRP-C6. It should be noted that, without the BS^3 cross linker, we failed to achieve the effective amplification in the QCM response.

3. Results and Discussion

3.1. Antigen-antibody kinetics

Figure 3(a) shows the binding curves for the CRP-immobilized three channels when the ACRP-C6 solution was injected. We evaluated the dissociation constant K_D between them from the binding and dissociating curves, yielding $K_D = 5.6$ nM. We obtained similar results in injecting the ACRP-C2 solution, confirming high binding affinity of the antibodies with CRP. On the other hand, when we injected the ACRP-C2 solution after 10000 s from the injection of the ACRP-C6 solution (i.e. the resonator surfaces were fully covered by ACRP-C6), the frequencies were little changed as shown in Fig. 3(b), indicating negligible interaction between ACRP-C2 and ACRP-C6 (nonspecific interaction). Thus, these two antibodies are suitable for the sandwich assay.

It is important to note that the binding curves cannot be explained by a single exponential curve but by two exponential curves as shown in Fig. 3(c). This can be attributed to the steric-hindrance effect: The frequency decrement at which the binding curve departs from the first exponential curve is about 100-150 ppm, and the Sauerbrey equation [16] estimates the number of attached antibody molecules of 2.1-3.2 mol on both quartz surfaces. This

corresponds to the average distance between nearby captured antibodies of 7.5-9.2 nm. According to the three-dimensional structure of an IgG molecule, dimensions of a single IgG is about $14 \times 9 \times 5 \text{ nm}^3$ [17] and the diameter of the equivalent sphere becomes about 11 nm, which is close to the average distance between nearby captured antibodies. Therefore, the resonator surfaces are covered by the antibody molecules at this stage and the adsorption activity deteriorates since then because of the steric-hindrance effect.

3.2. CRP detection

Figure 4 shows binding curves when we inject the mass-amplified ACRP-C6/ZZ-BNC solution on resonators, which were exposed to various-concentration CRP solutions in advance. (The numbers in the figure indicates the concentration of the CRP solution.) The resonance frequency decreases significantly for the resonator chip exposed to CRP when we inject the mass-amplified solution, but the frequency change is much smaller when we inject the ACRP-C6 only. Thus, the response amplification works remarkably. Figure 5(a) shows the relationship between the CRP concentration and the frequency change at 10000 s from the injection. The frequency change is largely amplified using the mass amplification with ZZ-BNC, achieving the the detection limit of 10 pg/ml or less. Even at shorter time (60 min), the detection limit is below 100 pg/ml (Fig. 5(b)). Previously, mass-amplified sandwich measurements with QCM were proposed for detecting CRP using gold nanoparticles [9] and streptavidin [11]. Their detection limits are 20 ng/ml and 100 pg/ml, respectively, to which the proposed method in this study is superior.

We used the cross-linker (BS³) for enhancing the binding strength between the Z-domain on ZZ-BNC and ACRP-C6, without which we failed to observe any amplification. This will be caused by higher affinity between ACRP-C6 and CRP than between ACRP-C6 and protein-A Z domain. The dissociate constant between IgG and protein A in this study is estimated to be about $K_D=1.6 \times 10^{-7} \text{ M}$ [18], which is much larger than that between CRP and ACRP-C6. Therefore, the ACRP-C6 molecules will be captured by CRP, causing detachment from the ZZ-BNC without the cross-linker.

There are various sandwich methods, and some of them show better detection sensitivity as seen in a review [19]. For example, Vance and Sandros [20] achieve a detection limit of 5 fg/ml in detecting CRP by capturing them with the CRP-specific aptamer and injecting the CRP-specific-aptamer-modified quantum dots, where the surface-plasmon-resonance response is significantly amplified. However, because the instrument compactness of QCM biosensor

has maintained superiority over other methods, progress in the mass amplified method proposed in this study will be important in the biosensor field.

4. CONCLUSION

The mass-amplified sandwich assay with ZZ-BNC was performed using the wireless high-frequency multichannel QCM biosensor. The fundamental resonance frequencies of the QCM resonator (54-60 MHz) were significantly higher than those in conventional QCM biosensors. The bonding between the Z-domains on ZZ-BNC and the anti-CRP detection antibody was strengthened by the cross-linker (BS³), which was necessary for making the effective signal amplification. The detection limit is 10 pg/ml, which is better than those of other sandwich methods with QCM. This value will be further improved by applying this method to ultrahigh-frequency (ultra-sensitive) wireless QCM biosensors. Currently, the detection time is not short enough. This will be caused by the steric-hinderance effect among BNCs, which deteriorates their binding affinity to the targets. Optimization of running buffer and number of immobilized antibody molecules on the surface will improve the detection time, which will be our future study.

ACKNOWLEDGEMENT

This study was partially supported by the Development of Advanced Measurement and Analysis Systems from Japan Science and Technology Agency, JST.

- [1] H. Muramatsu, M.D. Dicks, E. Tamiya, I. Karube, Piezoelectric crystal biosensor modified with protein A for determination of immunoglobulins, *Anal. Chem.* 59 (1987) 2760-2763.
- [2] Y. Liu, X. Yu, R. Zhao, D. Shangguan, Z. Bo, G. Liu, Quartz crystal biosensor for real-time monitoring of molecular recognition between protein and small molecular medicinal agents, *Biosens. Bioelectron.* 19 (2003) 9-19.
- [3] H. Ogi, K. Motohisa, T. Matsumoto, K. Hatanaka, M. Hirao, Isolated electrodeless high-frequency quartz crystal microbalance for immunosensors, *Anal. Chem.* 78 (2006) 6903-6909.
- [4] H. Ogi, Wireless-electrodeless quartz-crystal-microbalance biosensors for studying interactions among biomolecules: A review, *Proc. Jpn. Acad. Ser. B* 89 (2013) 401-417.
- [5] E. Uttenthaler, M. Schräml, J. Mandel, S. Drost, Ultrasensitive quartz crystal microbalance sensors for detection of M13-Phages in liquids, *Biosens. Bioelectron.* 16 (2001) 735-743.
- [6] H. Ogi, H. Nagai, Y. Fukunishi, M. Hirao, M. Nishiyama, 170-MHz Electrodeless Quartz Crystal Microbalance Biosensor: Capability and Limitation of Higher Frequency Measurement, *Anal. Chem.* 81 (2009) 8068-8073.
- [7] B. P. Stehrer, R. Schwödauer, S. Bauer, I. M. Graz, P. D. Pollheimer, H. J. Gruber, High frequency QCM based sensor system for sensitive detection of dissolved analytes, *Proc. Eng.* 5 (2010) 835-837.
- [8] Q. Chen, W. Tang, D. Wang, X. Wu, N. Li, F. Liu, Amplified QCM-D biosensor for protein based on aptamer-functionalized gold nanoparticles, *Biosens. Bioelectron.* 26 (2010) 575-579.
- [9] P. Ding, R. Liu, S. Liu, X. Mao, R. Hu, Reusable gold nanoparticle enhanced QCM immunosensor for detecting C-reactive protein, *Sens. Actuat. B* 188 (2013) 1277-1283.
- [10] J. Ding, Z. Lu, R. Wang, G. Shen, L. Xiao, Piezoelectric immunosensor with gold nanoparticles enhanced competitive immunoreaction technique for 2,4-dichlorophenoxyacetic acid quantification, *Sens. Actuat. B* 193 (2014) 568-573.

- [11] H. Ogi, T. Yanagida, M. Hirao, and M. Nishiyama, Replacement-Free Mass-Amplified Sandwich Assay with 180-MHz Electrodeless Quartz-Crystal Microbalance Biosensor, *Biosen. Bioelectron.* 26 (2011) 4819-4822.
- [12] M. Iijima, H. Kadoya, S. Hatahira, S. Hiramatsu, G. Jung, A. Martin, J. Quinn, J. Jung, S.-Y. Jeong, E. K. Choi, T. Arakawa, F. Hinako, M. Kusunoki, N. Yoshimoto, T. Niimi, K. Tanizawa, S. Kuroda, Nanocapsules incorporating IgG Fc-binding domain derived from *Staphylococcus aureus* protein A for displaying IgGs on immunosensor chips, *Biomate.* 32 (2011) 1455-1464.
- [13] M. Iijima, M. Somiya, N. Yoshimoto, T. Niimi, S. Kuroda, Nano-visualization of oriented-immobilized IgGs on immunosensors by high-speed atomic force microscopy, *Sci. Rep.* 2 (2012) 790.
- [14] H. Ogi, H. Nagai, Y. Fukunishi, T. Yanagida, M. Hirao, and M. Nishiyama, Multichannel Wireless-Electrodeless Quartz-Crystal Microbalance Immunosensor, *Anal. Chem.* 82 (2010) 3957-3962.
- [15] H. Ogi, K. Okamoto, H. Nagai, Y. Fukunishi, and M. Hirao, Replacement-Free Electrodeless Quartz Crystal Microbalance Biosensor Using Nonspecific-Adsorption of Streptavidin on Quartz, *Anal. Chem.* 81 (2009) 4015-4020.
- [16] G. Sauerbrey, Verwendung von Schwingquarzen zur Wägung dünner Schichten und zur Mikrowägung, *Z. Phys.* 155 (1959) 206-222.
- [17] V. R. Sarma, E. W. Silverton, D. R. David, W. D. Terry, The Three-Dimensional Structure at 6 Å Resolution of a Human γ G1 Immunoglobulin Molecule, *J. Biol. Chem.* 246 (1971) 3753-3759.
- [18] H. Ogi, K. Motohisa, K. Hatanaka, T. Ohmori, M. Hirao, M. Nishiyama, Concentration dependence of IgG-protein A affinity studied by wireless-electrodeless QCM, *Biosens. Bioelectron.* 22 (2007) 3238-3242.
- [19] P. Salvo, V. Dini, A. Kirchain, A. Janowska, T. Oranges, A. Chiricozzi, T. Lomonaco, F. D. Francesco, M. Romanelli, Sensors and Biosensors for C-Reactive Protein, Temperature and pH, and Their Applications for Monitoring Wound Healing: A Review, *Sensors* 17 (2017) 2952.

- [20] S. A. Vance, M. G. Sandros, Zeptomole Detection of C-Reactive Protein in Serum by a Nanoparticle Amplified Surface Plasmon Resonance Imaging Aptasensor, *Sci. Rep.* 4 (2014) 5129.

Figure Caption

Fig. 1 Schematic of wireless multichannel QCM biosensor.

Fig. 2 Illustrations of (a) mass-amplified detection antibodies with ZZ-BNC and (b) amplification mechanism.

Fig. 3 (a) Resonance frequency changes simultaneously measured by the multichannel wireless QCM in injection of 10 $\mu\text{g}/\text{ml}$ anti-CRP antibody C6 (ACRP-C6) solution, where CRP molecules are immobilized on the three resonator surfaces. (b) Resonance frequency changes in injection of 10 $\mu\text{g}/\text{ml}$ anti-CRP antibody C2 (ACRP-C2) solution after flow of the ACRP-C6 for 10000 s. (c) Resonance frequency changes in injections of the ACRP-C6 and ACRP-C6 solutions. The broken lines denote fitted exponential functions.

Fig. 4 Resonance frequency changes observed when the mass-amplified ACRP-C6 with ZZ-BNC solutions are injected (solid line) and that when the 10 $\mu\text{g}/\text{ml}$ ACRP-C6 solution is injected without mass amplification (broken line). The numbers indicate the CRP concentration of the CRP solution, in which the resonators were immersed in advance.

Fig. 5 (a) Relationship between CPR concentration and the frequency change at 10000 s, and (b) that at 3600 s.

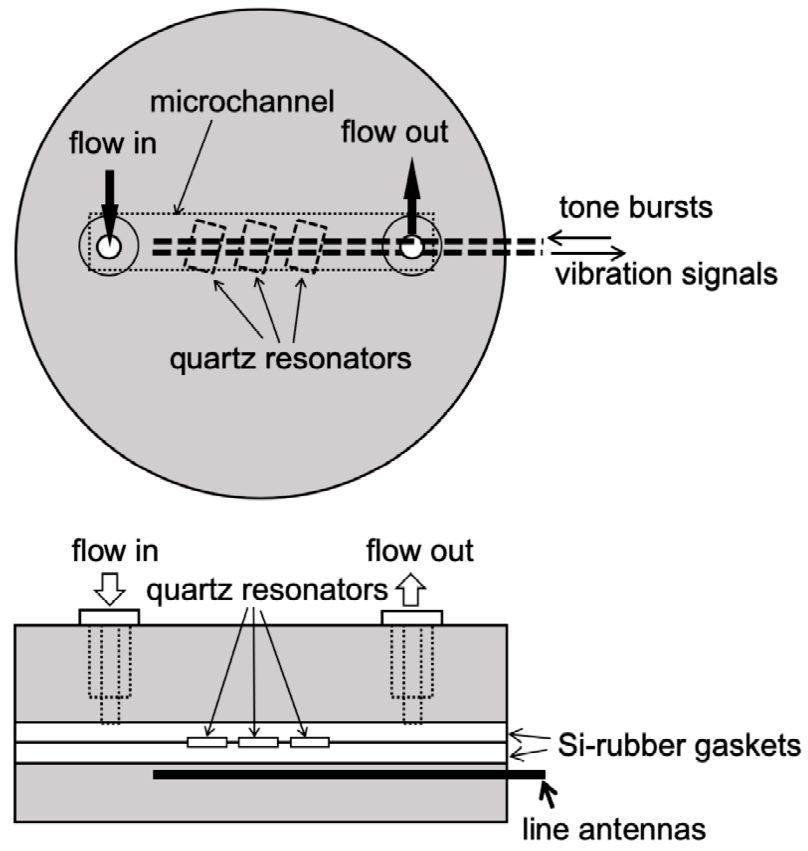


Figure 1:

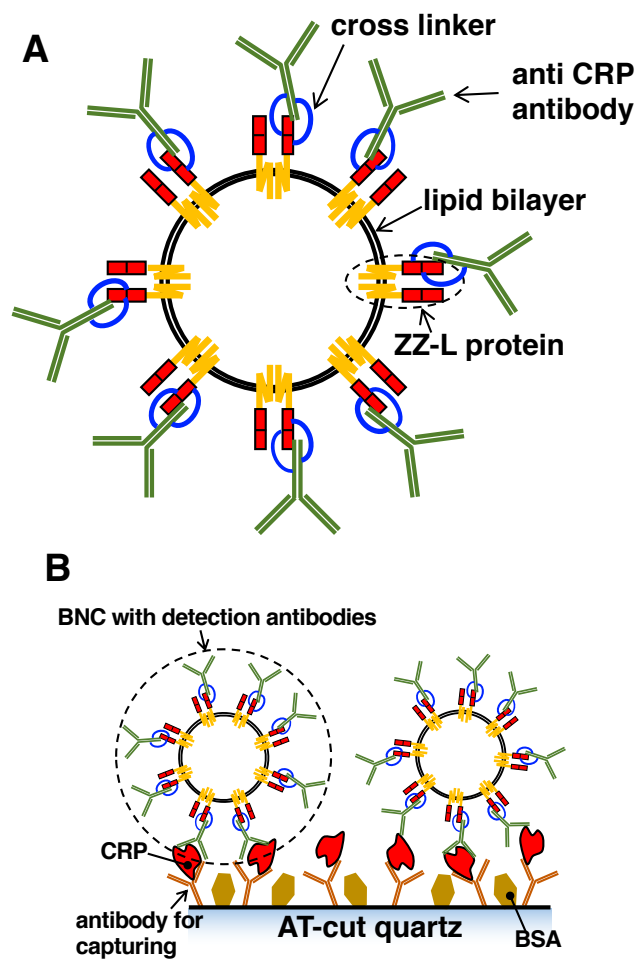


Figure 2:

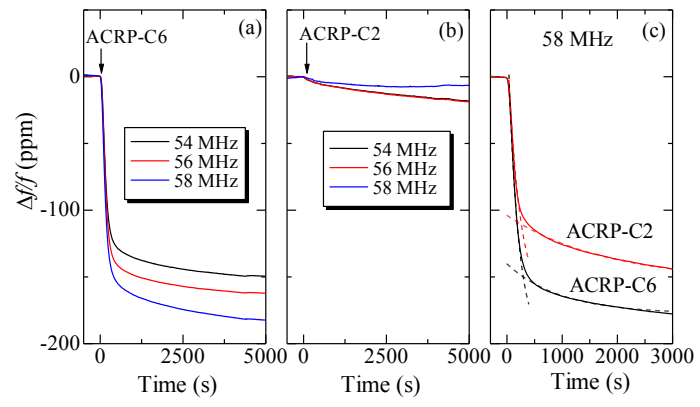


Figure 3:

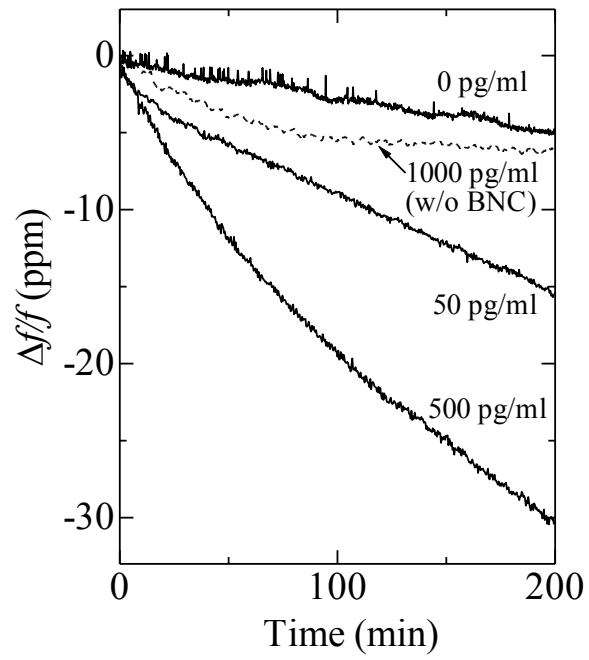


Figure 4:

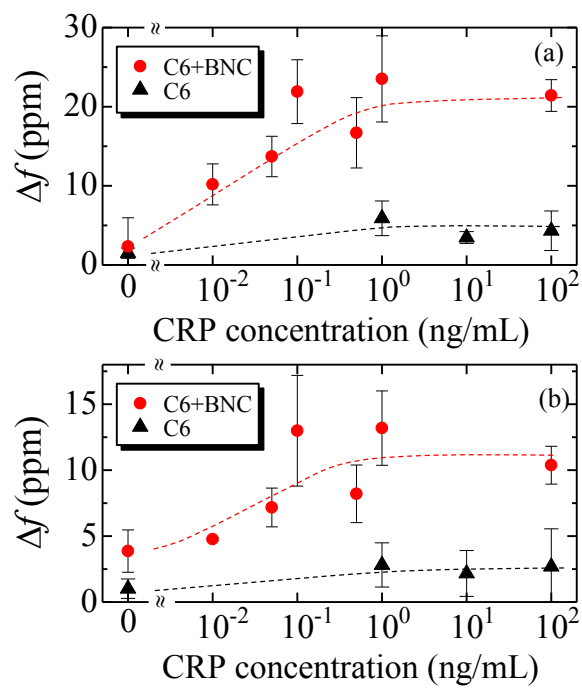
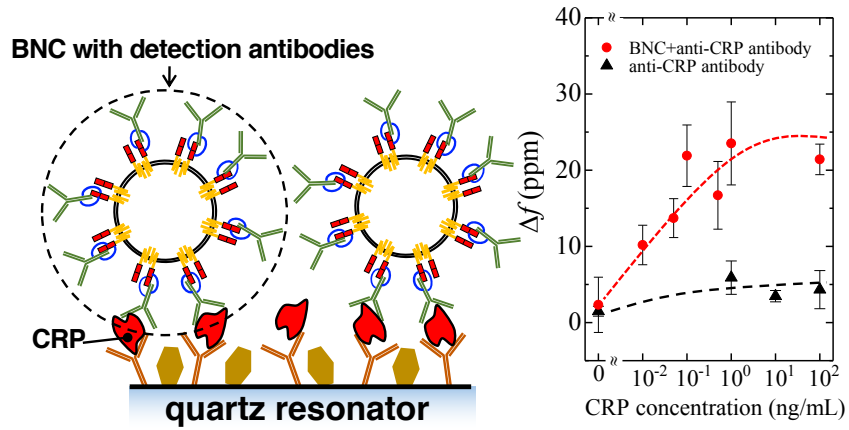


Figure 5:



Graphical Abstract